12.6 FULLY COUPLED "ONLINE" CHEMISTRY WITHIN THE WRF MODEL

Georg A. Grell[1]*, Steven E. Peckham[1], Rainer Schmitz[3], and Stuart A. McKeen[2]

[1]Cooperative Institute for Research in Environmental Sciences (CIRES),
University of Colorado/NOAA Research-Forecast Systems Laboratory, Boulder, Colorado
[2]Cooperative Institute for Research in Environmental Sciences (CIRES),
University of Colorado/NOAA Research – Aeronomy Laboratory, Boulder, Colorado
[3]Department of Geophysics, University of Chile, Santiago, Chile
Institute for Meteorology and Climate Research, Atmospheric Environmental Research (IMK-IFU),
Forschungszentrum Karslruhe, Garmisch-Partenkirchen, Germany

1. INTRODUCTION

The simulation and prediction of air quality is a complicated problem, involving both meteorological factors (such as wind speed and direction, turbulence, radiation, clouds, precipitation) and chemical processes (such as emissions, deposition, transformations). In the real atmosphere, the chemical and physical processes are coupled. The chemistry can affect the meteorology, for example, through its effect on the radiation budget, as well as the interaction of aerosols with Cloud Condensation Nuclei (CCN). Likewise, clouds and precipitation have a strong influence on chemical transformation and removal processes, and localized changes in the wind or turbulence fields affect the chemical transport on a continuous basis.

Until recently, the chemical processes in air quality modeling systems were usually treated independently of the meteorological model (as in CMAQ; Byun and Ching, 1999); (i.e., "***offline***"), except that the transport was driven by output from a meteorological model, typically available once or twice per hour. Due to this separation of meteorology and chemistry, there can be a loss of important information about atmospheric processes that quite often have a time scale of much less than the output time of the meteorological model, e.g., wind speed and direction, rainfall, and cloud formation. This may be especially important in air quality prediction systems, in which horizontal grid-sizes on the order of 1km may be required. In addition, the feedback from the chemistry to the meteorology – which is neglected in "offline" approaches – may be much more important than previously thought.

Over the past few years, several research institutes have collaborated in the development of a new state-of-the-art Weather Research and Forecast (WRF) model(http://www.mmm.ucar.edu/wrf/users/document.html). WRF is non-hydrostatic, with several dynamic cores as well as many different choices for physical parameterizations to represent processes that cannot be resolved by the model. This allows the model to be applicable on many different scales. The dynamic cores include a fully mass- and scalar-conserving flux form mass coordinate version, which represents a major improvement over commonly used non-hydrostatic models. Similar approaches have recently been implemented in the Operational Multiscale Environment Model with Grid Adaptivity (OMEGA, Bacon et al., 2002) as well as the Japanese numerical weather prediction model (Satoh, 2002). A fully conservative flux-form treatment of the equations of motion may be especially important for air quality applications. This makes the WRF model ideally suited to be the cornerstone for a next generation air quality prediction system.

"The Workshop on Modeling Chemistry in Cloud and Mesoscale Models", a first step towards the implementation of chemistry into WRF, was held at NCAR on 6-8 March 2000. The

goal of this workshop was to produce a community assessment of approaches and methodologies used for chemistry modeling in cloud and mesoscale models. Since then, various chemical modules have been implemented into the WRF framework, creating an "online" WRF/chem model. Transport of species is done using the same vertical and horizontal coordinates (no horizontal or vertical interpolation), the same physics parameterization, and no interpolation in time. This WRF/Chem model is similar in its physical and chemical concepts to MM5/Chem (Grell et al. 2000). We will describe the chemical aspects of the model in section 2. In section 3 we will explain the setup for retrospective runs that were used for initial model evaluation. Section 4 will give results, and section 5 will provide a summary.

2. MODEL DESCRIPTION

In general, most air quality modeling systems consider a variety of coupled physical and chemical processes such as transport, deposition, emission, chemical transformation, aerosol interactions, photolysis, and radiation. Details on the modules that describe these processes within WRF/chem are given below. For details describing the conservative split-explicit time integration method that is used in the mass coordinate version of the WRF model, the reader is referred to http://www.mmm.ucar.edu/individual/skamarock/wrf_equations_eulerian.pdf. The time splitting method is described in Wicker and Skamarock (2002), and an overview of the physics is given in http://www.mmm.ucar.edu/wrf/users/wrf-doc-physics.pdf. Here we will only discuss the aspects of the model that directly relate to the chemical part.

2.1 Transport

All transport of chemical species is done "online". Although WRF has several choices for dynamic cores, for this paper we chose the official mass coordinate version of the model. For the mass coordinate WRF model this means the advection is fully mass and scalar conserving, fifth order in space, and third order in time. Turbulent transport is done using a level 2.5 Mellor-Yamada closure (ETA scheme).

For the chemical mechanism used in this version of the model, 39 chemical species are fully prognostic. For the aerosol module (see description below), another 34 variables are added, including the total number of aerosol particles within each mode, as well as all primary and secondary species (organic and inorganic) for both Aitken and accumulation mode, and three species for the coarse mode (anthropogenic, marine, and soil-derived aerosols).

2.2 Dry Deposition

The flux of trace gases and particles from the atmosphere to the surface is calculated by multiplying concentrations in the lowest model layer by the spatially and temporally varying deposition velocity, which is proportional to the sum of three characteristic resistances (aerodynamic resistance, sublayer resistance, surface resistance). The surface resistance parameterization developed by Wesely (1989) is used. In this parameterization, the surface resistance is derived from the resistances of the surfaces of the soil and the plants. The properties of the plants are determined using landuse data and the season. The surface resistance also depends on the diffusion coefficient, the reactivity, and water solubility of the reactive trace gas.

The dry deposition of sulfate is described differently. In case of simulations without calculating aerosols explicitly, sulfate is assumed to be present in the form of aerosol particles, and its deposition is described according to Erisman et al. (1994).

When employing the aerosol parameterization, the deposition velocity,

$\hat{v}_{dk}$, for the *k*th moment of a polydisperse aerosol is given by

$$\hat{v}_{dk} = (r_a + \hat{r}_{dk} + r_a \hat{r}_{dk} \hat{v}_{Gk})^{-1} + \hat{v}_{Gk}$$

where r_a is the surface resistance, $\hat{v}_{Gk}$ is the polydisperse settling velocity, and r_{dk} is the Brownian diffusivity (Slinn and Slinn, 1980; Pleim et al., 1984).

2.3 Gas-phase chemistry

This atmospheric chemical mechanism was originally developed by Stockwell et al. (1990) for the Regional Acid Deposition Model, version 2 (RADM2) (Chang et al., 1989). The RADM2 mechanism is a compromise between chemical detail, accurate chemical predictions, and available computer resources. It is widely used in atmospheric models to predict concentrations of oxidants and other air pollutants.

Inorganic species included in the RADM2 mechanism are 14 stable species, 4 reactive intermediates, and 3 abundant stable species (oxygen, nitrogen and water). Atmospheric organic chemistry is represented by 26 stable species and 16 peroxy radicals. The RADM2 mechanism represents organic chemistry through a reactivity aggregated molecular approach (Middleton et al., 1990). Similar organic compounds are grouped together into a limited number of model groups through the use of reactivity weighting. The aggregation factors for the most emitted Volatile Organic Compounds (VOCs) are given in Middleton et al., (1990).

A quasi steady state approximation method with 22 diagnosed, 3 constant and 38 predicted species is used for the numerical solution. The rate equations for 38 predicted species are solved using a Backward Euler scheme.

2.4 Biogenic Emissions

WRF/chem uses a biogenic emission module based on the description of Guenther et al. (1993, 1994), Simpson et al. (1995), and Schoenemeyer et al. (1997). The module treats the emissions of isoprene, monoterpenes, Other VOC (OVOC), and nitrogen emission by the soil. For the use in the RADM2 photochemistry module, the emissions of monoterpenes and OVOC are disaggregated into the RADM2 species classes.

The emission of isoprene by forests depends on both temperature and photosynthetic active radiation. Guenther et al. (1993) have developed a parameterization formula for the isoprene emission, where the isoprene emission rate is proportional to the isoprene emission rate at a standard temperature and a standard flux of photosynthetic active radiation. A radiation flux correction term and a temperature correction term for forest isoprene emissions is applied. The isoprene emissions of agricultural and grassland areas are considered to be functions of the temperature only (Hahn et al. 1994).

The emissions of monoterpenes, OVOC, and nitrogen are also treated as functions of the temperature only. Little is known about the emission of OVOC; therefore the same temperature correction is applied for OVOC as for monoterpenes according to Simpson et al. (1995).

The emissions at the standard temperature and the standard PAR flux are given in Table 1 in Grell et al. (2000). They are taken from Guenther et al. (1994) for deciduous, coniferous and mixed forest and from Schoenemeyer et al. (1997) for agricultural and grassland. For the use with RADM2, all nitrogen emissions are treated as NO. This is a maximum estimate, because the emission of N_2O is neglected.

It must be noted that from the landuse categories used in WRF, the nature of biogenic emissions can be estimated only roughly. Segregation into tree species will be necessary. Furthermore the fractional coverage of these species per single grid square will be required in the future.

2.5 Parameterization of Aerosols

The aerosol module is based on the Modal Aerosol Dynamics Model for Europe (MADE) (Ackermann et al., 1998) which itself is a modification of the Regional Particulate Model (Binkowski and Shankar, 1995). Secondary Organic Aerosols (SOA) have been incorporated into MADE by Schell et al., (2001), by means of the Secondary Organic Aerosol Model (SORGAM). Since the different components of the module are well documented in the above cited references, only a brief summary of the most important features shall be given here.

2.5.1 Size distributions

The size distribution of the submicrometer aerosol is represented by two overlapping intervals, called modes, assuming a log-normal distribution within each mode:

$$n(\ln d_p) = \frac{N}{\sqrt{2\pi}\ln\sigma_g}\exp\left[-\frac{1}{2}\frac{(\ln d_p - \ln d_{pg})^2}{\ln^2\sigma_g}\right],$$

where N is the number concentration [m^{-3}], d_p the particle diameter, d_{pg} the median diameter, and σ_g the standard deviation of the distribution. The kth moment of the distribution is defined as

$$M_k = \int_{-\infty}^{\infty} d_p^k n(\ln d_p) d(\ln d_p),$$

with the solution

$$M_k = N d_{p_g}^k \exp\left[\frac{k^2}{2}\ln^2\sigma_g\right].$$

M_0 is the total number of aerosol particles within the mode suspended in a unit volume of air, M_2 is proportional to the total particulate surface area within the mode suspended in a unit volume of air, and M_3 is proportional to the total particulate volume within the mode suspended in a unit volume of air.

2.5.2 Nucleation, Condensation, and Coagulation

The most important process for the formation of secondary aerosol particles is the homogeneous nucleation in the sulfuric acid-water system. It is calculated by the method given by Kulmala *et al.* (1998).

Aerosol growth by condensation occurs in two steps: the production of condensable material (vapor) by the reaction of chemical precursors, and the condensation and evaporation of ambient volatile species on aerosols. In MADE the Kelvin effect is neglected, allowing the calculation of the time rate of change of a moment M_k for the continuum and free-molecular regime. The mathematical expressions of the rates and their derivation are given in Binkowski and Shankar (1995).

During the process of coagulation, the distributions remain log-normal. Furthermore, only the effects caused by Brownian motion are considered for the treatment of coagulation. The mathematical formulation for the coagulation process can be found in Whitby et al. (1991), and Binkowski and Shankar (1995).

The change in moments due to coagulation is modified from that described by Whitby et al. (1991). Whereas Whitby et al. (1991) suggest that the collisions of particles within a mode result in the formation of a particle within that mode, MADE allows a particle resulting from two particles colliding within the Aitken mode to be assigned to the accumulation mode. For this, MADE calculates the diameter, d_{eq}, at which the two modes have equal number concentrations. Colliding particles in the Aitken mode, where at least one exceeds this diameter, are then assigned to the accumulation mode.

2.5.3 Aerosol Chemistry

The inorganic chemistry system is based on MARS (Saxena et al., 1986) and its modifications by Binkowski and Shankar (1995), which calculates the chemical composition of a sulphate-nitrate-

ammonium-water aerosol according to equilibrium thermodynamics. Two regimes are considered depending upon the molar ratio of ammonium and sulphate. For values less than 2, the code solves a cubic polynomial for hydrogen ion molality, and if enough ammonium and liquid water are present, it calculates the dissolved nitrate. For modal ionic strengths greater than 50, nitrate is assumed not to be present. For molar ratios of 2 or greater, all sulphate is assumed to be ammonium sulphate and a calculation is made for the presence of water. The Bromley method is used for the calculation of the activity coefficients.

The organic chemistry is based on SORGAM (Schell et al., 2001). SORGAM assumes that SOA compounds interact and form a quasi-ideal solution. The gas/particle portioning of SOA compounds are parameterized according to Odum et al. (1996). Due to the lack of information, all activity coefficients are assumed to be unity. SORGAM treats anthropogenic and biogenic precursors separately, and may be used with a chemical mechanism such as RACM (Stockwell et al. 1997) that provides the biogenic precursors. Since in WRF/chemistry we currently use the RADM2 mechanism (Stockwell et al., 1990), the biogenic precursors and their resulting particle concentrations are set to zero.

2.5.4 Interaction with atmospheric radiation

The interaction of aerosols and radiation has been incorporated by means of a simplified parameterization into the short wave radiation scheme (Dudhia, 1989). This parameterization only takes into account three variables: elemental carbon, dry aerosol mass (without elemental carbon), and aerosol liquid water content. Only absorption is considered for elemental carbon, whereas for dry aerosol mass and aerosol liquid water content, only scattering is considered. This parameterization is not spectrally dependent, nor does it, at this stage, take into account the aerosol size and asymmetry dependency on radiation.

2.6 Photolysis frequencies

Photolysis frequencies for the 21 photochemical reactions of the gas phase chemistry model are calculated at each grid point according to Madronich (1987). The photolysis frequency of the gas *i*, J_i, is given by the integral of the product of the actinic flux I_A (λ), the absorption cross sections σ (λ), and the quantum yields Φ (λ) over the wavelength λ:

$$J_i = \int^{\lambda} I_A(\tau,\lambda)\sigma_i(\lambda)\Phi_i(\lambda)d\lambda$$

For the calculation of the actinic flux, a radiative transfer model by Wiscombe which is based on the delta-Eddington technique (Joseph et al., 1976), is used. This radiative transfer model accounts for absorption by O_2 and O_3, Rayleigh scattering, and scattering and absorption by aerosol particles and clouds as described by Chang et al. (1989). The absorption cross sections and the quantum yields for the calculation of J_{gas} are given by Stockwell et al. (1990). The integral in the above equation is solved for 130 wavelengths between 186 and 730 nm.

The profiles of the actinic flux are computed at each grid point of the model domain. For the determination of the absorption- and scattering cross sections needed by the radiative transfer model, predicted values of temperature, ozone, and cloud liquid water content are used below the upper boundary of WRF. Above the upper boundary of WRF, fixed typical temperature and ozone profiles are used to determine the absorption and scattering cross sections. These ozone profiles are scaled with TOMS satellite observational data for the area and date under consideration.

The radiative transfer model permits the proper treatment of several cloud layers with height-dependent liquid water contents

each. The extinction coefficient of cloud water $ß_c$ is parameterized as a function of the cloud water computed by the 3-dimensional model based on a parameterization given by Slingo (1989). For the present study, the effective radius of the cloud droplets follows Jones et al. (1994). For aerosol particles a constant extinction profile with an optical depth of 0.2 is applied.

An online computation of the photolysis frequencies is preferred here since it has advantages over "offline" techniques and is more versatile. One advantage is that the absorption cross sections of ozone are temperature dependent. Furthermore this treatment can be used to account for the humidity dependence of the extinction by aerosol particles. As shown by Ruggaber et al. (1994), aerosol particles have a strong effect on the photolysis frequency of NO_2. Another possible option for the model is the parameterization of cloud droplets as a function of the sulfate content according to Jones et al. (1994).

The photolysis model may be applied at any timestep. However, for numerical efficiency, the photolysis routine is called with time intervals of 30 minutes.

3. TEST-BED SETUP

The air quality forecasting testbed concept envisions an extended period during which forecast models are continuously run and evaluated, punctuated by intense process studies where specific aspects of the forecasting problem are targeted and investigated. Here we evaluate WRF/chem over a two month period in summer of 2002. This period was previously used to evaluate the real-time performance of MM5/chem as well as other air quality models (McKeen et al. 2003). To be able to compare to the previous MM5/chem evaluation, the setup was chosen to be almost identical to the MM5/chem runs.

A series of 36-hour simulations are performed on a roughly 3600 km x 3000 km numerical grid having 27-km horizontal resolution and centered at 86°W longitude and 34.5°N latitude. The domain extends vertically to 18 km with a vertical mesh interval smoothly increasing from 7 m near the surface to approximately 500 meters at the domain top. Simulations are conducted every 12 hours (00Z and 12Z) starting from 5 July 2002 and ending on 20 August 2002. Information about the configuration of the WRF/chem model is provided in Table 1.

Meteorological initial conditions were obtained from the Rapid Update Cycle (RUC) model analysis fields generated at FSL, and lateral boundary conditions are derived from the NCEP ETA-model forecast. Atmospheric chemical constituents are initialized from the previous 12-hour forecast with the exception of the 00Z simulation for 5 July 2002 that uses an idealized atmospheric chemistry profile.

This idealized profile was also used to provide inflow lateral boundary conditions for the chemical fields.

Anthropogenic emissions were interpolated to the three-dimensional model grid and updated hourly. The anthropogenic surface and point source emissions used in the simulations are obtained from the EPA NET-96 emission database.

Table 1. WRF/Chem "online" Configuration options

Advection scheme	5^{th} horizontal /3^{rd} vertical
Microphysics	NCEP 3-class simple ice
Longwave radiation	RRTM
Shortwave radiation	Dudhia
Surface layer	Monin-Obukhov (Janjic Eta)
Land-surface model	OSU
Boundary layer scheme	Mellor-Yamada-Janjic TKE
Cumulus parameterization	Betts-Miller-Janjic
Chemistry option	RADM2
Dry deposition	Weseley 1989
Biogenic emissions	Gunther94 +Simpson95
Photolysis option	Madronich 1987
Aerosol option	MADE/SORGAM

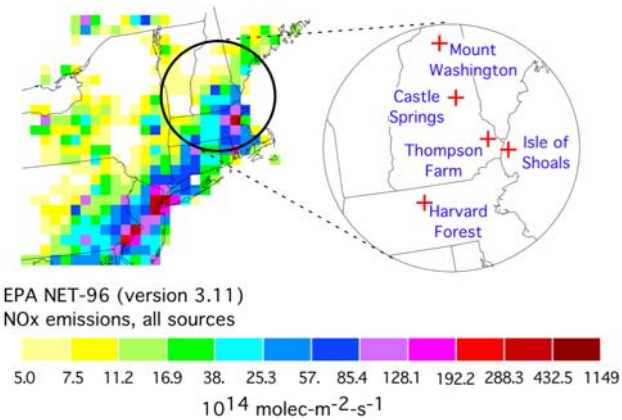

Figure 1. Diurnally averaged summertime weekday NOx emissions for the 27 km horizontal grid in the New England region, and the location of the five surface sites used in the statistical evaluation.

Fig. 1 illustrates the location of the surface observing sites that are used for the evaluations discussed below relative to the 27km emissions inventory of NOx. Details on the location and characteristics of the four surface sites can be found at internet address http://www.airmap.unh.edu/home. The elevations of Thomson Farm, Castle Springs, and Mount Washington sites are 75, 400 meters, and 1915 meters, respectively. Both model results and observations suggest a strong influence from the Boston region on the air quality at Thompson Farm and Isle of Shoals, a mixed source of urban coastal and more regional sources from the Boston-Washington corridor affecting the Castle Springs site, and except for nearby emissions from a cable-car and parking lot, only long range regional sources affecting the Mount Washington site. The Harvard Forest site has been collecting air quality data for more than a decade and is well characterized in terms of anthropogenic and natural sources and transport paths [e.g. Goldstein et al., 1995, Munger et al., 1998], as well as O_3 and related photochemistry [e.g. Hirsch et al., 1996]. Air quality at this site is most often impacted by southwesterly airflow from the New York City – Washington D.C. corridor.

The only PM2.5 data available for model comparison is at Thompson Farm. Gas-phase species directly comparable between the Air Quality Forecast Models (AQFMs) and the individual sites include CO and O_3 at Isle of Shoals, CO, O_3, NO, NOy and SO_2 at Thompson Farm and Castle Springs, and CO, O_3, NO, and SO_2 at the Mount Washington site. Data from the AIRMAP sites were archived on a one-minute time base, and hourly averages are calculated for comparisons with hourly snapshots of the model results. The Harvard Forest site archived hourly averaged CO, O_3, NOy, NO, NO_2 and PAN. Because of its short lifetime and extreme variability, comparisons between model and measured NO are not considered here. The time period of the statistical analysis extends from 00Z 13 July to 00Z 20 August, 2002. Each model had complete coverage during this period allowing 38 days of model-measurement overlap. Only data and model results for the 11:00 am to 7:00 pm EDT (15 to 23 UTC) are used in the analysis. These hours usually bracket the maximum diurnal O_3 concentrations at all the sites.

4.RESULTS

Fig. 2 shows an example of hourly averaged O_3 at Thompson Farm with the WRF/chem model results. The 15-23 hour forecasts correspond to the 00Z daily forecast, while the 3-11 hour forecasts correspond to the daily 12Z run of this particular model and resolution. There are 342 comparison points for each forecast lead time, allowing for high confidence in the statistics derived in these comparisons. Two statistical measures shown in Figure 2 are used to compare the various model forecasts; the Pearson's r^2 correlation coefficient as a measure of forecast skill, and the median error (model minus observation) as a measure of model bias. Determination of this latter quantity is illustrated in Fig. 2b for the three separate forecast lead times and the combined data set. Model errors are sorted, and the error at the midpoint of the sorted distribution is noted, along with the errors at the 1/6 and 5/6 quantiles to describe the error spread within the central 2/3 of the error distribution set.

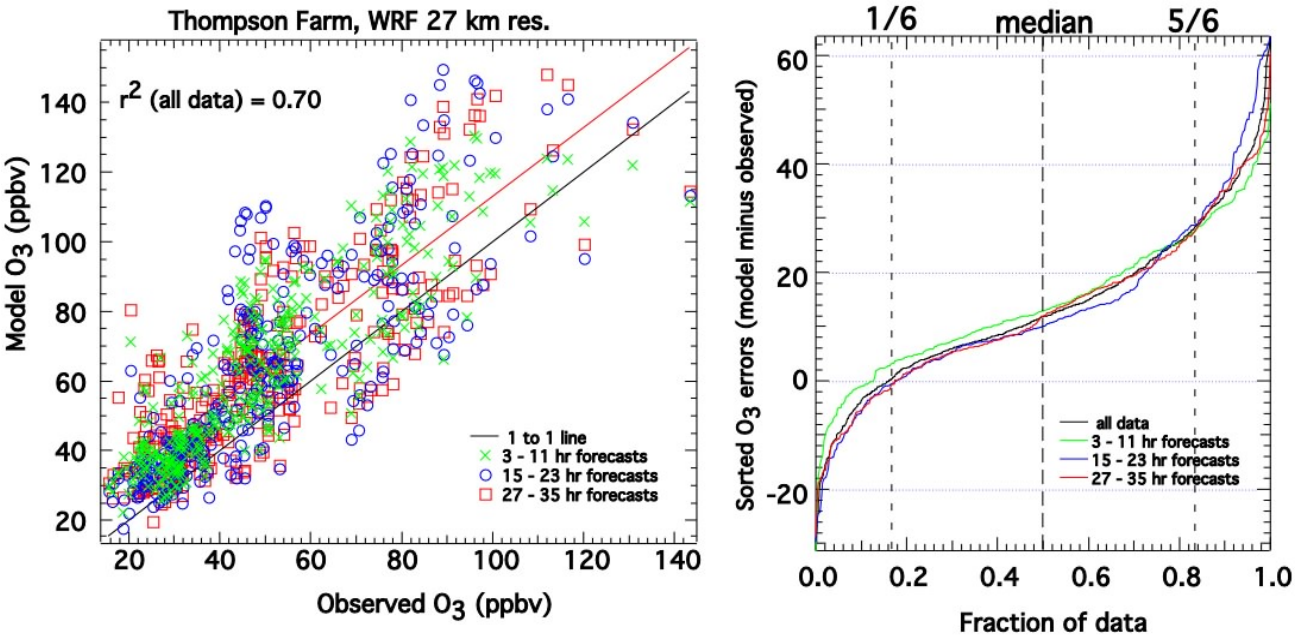

Figure 2. Scatter plot (a) of WRF/chem model versus observed O_3 at Thompson Farm, NH, between 7/13/02 and 8/20/02, windowed between 15:00 and 23:00 UTC hours. Observations are averaged over hourly intervals (coincident with model results). The red line is the regression line for the linear-least squares fit for all forecasts. Also shown is the distribution of model errors (b), sorted in ascending order from the data shown in Figure 2a. The dotted lines show the position of the 1/6 and 5/6 quantiles, the dashed line is at the median.

Some final caveats in the statistical comparisons should be noted. Because of intermittent outages and problems with data logging at Harvard Forest, only about two thirds of the total possible hourly averages are available. Because of the direct influence of the parking lot below Mount Washington, all one-minute samples with NO greater than 8 ppbv are removed from the analysis. Without this filter O_3 correlations with the models are essentially zero due to the O_3 titration effects.

The r^2 and median error statistics for all of the WRF/chem and MM5/chem O_3 predictions are summarized graphically in Fig. 3. For the MM5/chem model, results from all three model resolutions are shown for completeness. The r^2 coefficients derived from eight-hour averages are also included in these plots, as discussed further below. Several important aspects of the model statistics have been discussed in a report that compares the MM5/chem results with another AQFM (McKeen et al., 2003). The most relevant comparisons for the purposes of this study are between the WRF/chem results (shown as crosses), and the 27 km horizontal resolution MM5/chem results. For O_3, the WRF r^2 coefficients (based on hourly averages) are higher than those of MM5/chem for 12 out of the 15 possible lead-time/site combinations. Biases are generally indistinguishable between all of the model cases. One can conclude that the WRF/chem model exhibits improved model skill relative to MM5/chem for O_3. Although there is less confidence associated with the r^2 values derived from eight-hour averages (only 38 points in the linear regressions), they are always as large or larger than the r^2 values derived from one-hour averages. This implies that model/observation correlations at each site are driven by the models' ability to simulate large scale, day-to-day variability in O_3, as opposed to variability forced by processes acting over timescales from one to several hours.

Unlike O_3, NOy has negligible photochemical sources, and provides a more direct link between anthropogenic source regions and transport to the various sites.

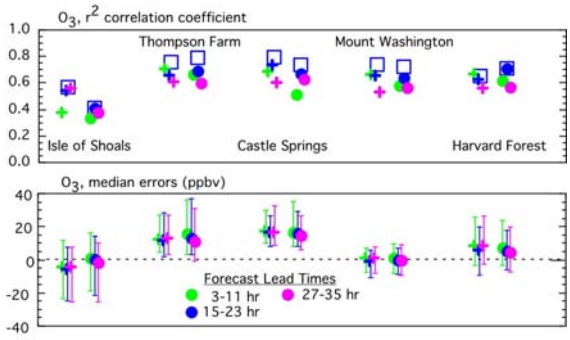

Figure 3: Summary statistics (r^2 correlation coefficients, and median errors with bars showing 1/6 and 5/6 quantiles) for O_3 at the four AIRMAP sites and Harvard Forest. Data have been windowed for comparisons between 15:00 and 23:00 UTC hours from 7/13/02 and 8/20/02. The abscissa shows the five stations with some small scatter to distinguish the various forecast lead times (green – 3 to 11 hours, blue – 15 to 23 hr, purple – 27 to 35 hr, red – 39 to 47 hr). MM5/chem results are solid filled circles (hourly averages used in comparisons), crosses correspond to the WRF/chem. The squares are statistics for the 8 hour (15:00 and 23:00 UTC) averages of the 15 to 23 hr lead-time forecast.

Fig. 4 shows the statistical measures for NOy for those surface sites with NOy measurements. In the case of NOy, sorted distributions of observations and model results generally conform to a log-normal distribution rather than just a normal distribution. For this reason, Pearson r^2 values of the log-transformed mixing ratios are used as a measure of forecast skill, and median values of sorted distributions of the model/observation ratio are used as the measure of model bias. The patterns for the NOy statistical measures for the hourly averages show that 8 out of 9 lead-time/site combinations show improved r^2 values with WRF/chem compared to MM5/chem. All model cases overpredict NOy by a factor of two or more at the Thompson Farm and Harvard Forest, which could be due to coarse spatial partitioning in the emissions inventory, inefficient vertical mixing and dispersion, or the partitioning of NOy into forms of odd-nitrogen other than HNO_3 (which is efficiently removed by surface deposition). However, at all sites, the WRF/chem model is biased higher than MM5/chem model. The most likely cause of this persistent model difference is related

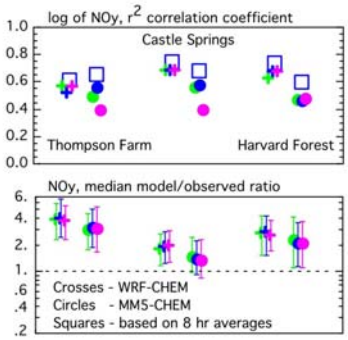

Figure 4: As in Figure 3, except for NOy. Because of log-normal distributions in NOy concentrations and model errors, Pearson r^2 correlation coefficients are from logarithms of mixing ratios, and biases are represented by median model/observed ratios.

to the parameterizations of the PBL physics used in the two formulations, specifically with respect to the parameterization of the surface fluxes and the way that they are coupled to the boundary layer. The fact that O_3 (photochemically produced well above the surface) does not show a difference in model bias, but NOy (primary sources from surface emissions) does show a difference (CO showed the same behaviour as NOy, but is not shown here), suggests that upward transport out of the bottom few model layers is sufficiently different between the models to affect the statistics. This further implies that the PBL physics parameterization applied to chemical constituents within these air quality models should be reviewed and validated with appropriate measurements and numerical testing.

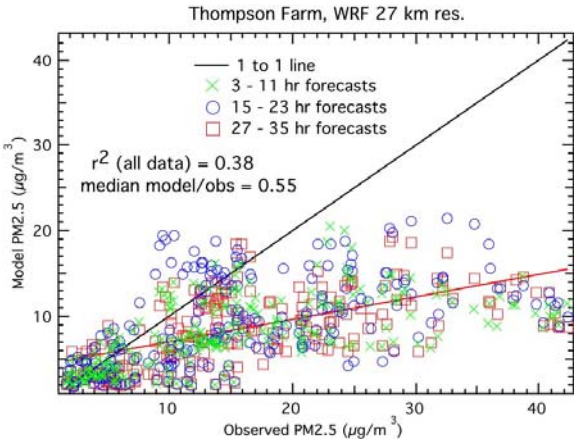

Figure 5: As in Figure 2, except for PM2.5

	1 hour averages				8 hour averages		
	r^2	Model-obs Median	1/6 and 5/6 quantiles		r^2	Model-obs Median	1/6 and 5/6 quantiles
O_3							
WRF/chem	0.57	-0.2	-14/12		0.60	-1.1	-11/10
MM5/chem	0.36	2.7	-17/19		0.41	1.3	-16/14
	r^2 of logs	Model/obs Median ratio	1/6 and 5/6 quantiles		r^2 of logs	Model/obs Median ratio	1/6 and 5/6 quantiles
NOy							
WRF/chem	0.32	3.0	1.4 / 9.0		0.58	2.7	1.5 / 5.2
MM5/chem	0.33	2.3	1.0 / 6.4		0.59	1.9	1.1 / 4.6
SO_2							
WRF/chem	0.22	4.1	0.7/11.6		0.51	2.9	0.8 / 6.6
MM5/chem	0.29	1.6	0.3 / 7.4		0.52	1.9	0.6/4.6

Table 2; Summary statistics for comparisons between WRF and MM5 chemistry models with observations collected on the RV Ron Brown between 7/14/02 to 8/7/02, and excluding 8/6/02. Model/observation comparisons are only done for the 15Z to 23Z time periods. Only statistics for the 00Z forecast (15 to 23 hour forecast lead time) are shown.

Fig. 5 shows a scatter plot of hourly averaged PM2.5 from the model and the observations. There is clearly a correlation between the model and observations, particularly at the high end. However, the median model PM2.5 under-prediction is 55%. The major source of model PM2.5 mass is from unspeciated primary emissions, rather than the condensation of gas-phase inorganic and organic species. The shallow slope of the linear regression (0.26) shown in Figure 5 suggests that either PM2.5 emissions from the EPA-NET 96 inventory are too low, or that the model is not adequately treating the exchange of mass from the gas to aerosol phase during high pollution transport to this site. Further research on this issue is in progress. Additionally, model results will be compared to data from the Ron Brown.

To complete the surface site statistical analysis, Table 2 summarizes the forecast skill and model bias for SO_2 , O_3, and NOy from the two models and for NOAA's ship vessel Ron Brown. For the ship data the WRF/chem model shows significant improvement in skill for ozone, but none for NOy and SO_2; however biases of these species are higher than MM5/chem's. The NET-96 inventory of SO_2 is not expected to be representative of 2002 due to the implementation of controls at the highest SO_2 point sources in the Northeast U.S. between 1996 and 2002.

5. SUMMARY

Fully coupled, "online" chemistry has been implemented into the WRF model. The resulting WRF/chem model was then evaluated in comparison to MM5/chem with a test-bed data set. The results presented are a summary of statistical comparisons of atmospheric composition predicted by WRF/chem and MM5/chem. The photochemistry and emissions are

identical between the two models, allowing an examination of the effects of differences between the MM5 and WRF formulations on O_3 photochemical forecasts. Statistical analysis is based upon comparisons of model results with detailed photochemical data collected during the summer of 2002 field study. Analysis of variance and bias for five surface sites and ship-based measurements of O_3 and its precursors allow some important qualitative generalizations to be made. First, the WRF/chem model statistically shows better skill in forecasting O_3 than MM5/chem with no appreciable differences between models in terms of bias with the observations. Secondly, the WRF/chem model also consistently exhibits better skill at forecasting the O_3 precursors CO and NOy (except for the ship location). However, WRF/chem model biases of these precursors and photo-oxidants are persistently higher than for MM5/chem, and are most often biased high compared to observations. The reason behind the higher WRF/chem biases is probably related to differences in vertical transport between the two models, particularly with the treatment of the bottom few layers within the different PBL physics parameterizations. This points to the importance of vertical transport algorithms and transport rates within the air quality forecasts, and the need for verification of these transport algorithms with appropriate information regarding vertical structure and gradients. Lastly, when statistical analysis is applied to the 11 am to 7 pm averages of the model and measured data, forecast skill for O_3 and its precursors is always better than the same statistics based on hourly data for the same time periods. This suggests that forecast skill on all temporal scales is largely determined by the skill in predicting large scale, day-to-day meteorological variability. The improvement in the forecast skill of WRF/chem, though not always very large, is probably related to improved predictions of larger scale dynamics and physical meteorology within the WRF formalism.

6. ACKNOWLEDGEMENTS

The authors gratefully acknowledge the measurements of the AIRMAP network (University of New Hampshire), Harvard Forest (Bill Munger) and the NOAA RV Ron Brown (Eric Williams, Christof Senff) that contributed to this work. We are also grateful to Susan Carsten for editorial assistance, and Dezso Devenyi as well as Steven Koch for reviewing this manuscript..

7. REFERENCES

Ackermann, I. J., H. Hass, M. Memmesheimer, A. Ebel, F. S. Binkowski, and U. Shankar, 1998: Modal aerosol dynamics model for Europe: Development and first applications, *Atmos. Env.*, 32, No.17, 2981-2999.

Bacon, D. P., N. Ahmad, Z. Boybeyi, T. J. Dunn, M. S. Hall, P. C. S. Lee, R. A. Sarma, M. D. Turner, K. T. Waight, S. H. Young and J. W. Zack, 2000: A dynamically adapting weather and dispersion model: The Operational Multiscale Environment Model with Grid Adaptivity (OMEGA), *Mon. Wea. Rev.*, **128**, 2044–2076.

Binkowski, F. S. and U. Shankar, 1995: The regional particulate matter model, 1. Mode desription and preliminary results, *Journal of Geophysical Research*, **100**, 26191-26209.

Byun, D. W. and S. Ching (eds), 1999: Science algorithms of the EPA Models-3 Community Multiscale Air Quality (CMAQ) modeling system, EPA/600/R-99/030, U.S. EPA, Research Triangle Park, NC, March 1999.

Chang, J. S., F. S. Binkowski, N. L. Seaman, J. N. McHenry, P. J. Samson, W. R. Stockwell, C. J. Walcek, S. Madronich, P. B. Middleton, J. E. Pleim and H. H. Lansford, 1989: The regional acid deposition model and engineering model. *State-of-Science/Technology, Report 4,*

National Acid Precipitation Assessment Program, Washington D.C.

Dudhia, J, 1989: Numerical study of convection observed during winter monsoon experiment using a mesoscale two-dimensional model, *J. Atmos. Sci*. **46**, 3077-3107.

Erisman, J. W., A. van Pul, and P. Wyers, 1994: Parameterization of surface resistance for the quantification of atmospheric deposition of acidifying pollutants and ozone. *Atmos. Env.*, **28**, 2595-2607.

Goldstein, A.H., S.C. Wofsy, and C.M. Spivakovsky, 1995: Seasonal variations of nonmethane hydrocarbons in rural New England: Constraints on OH concentrations in northern midlatitiudes, J. Geophys. Res., 100, 21,023-21,033.

Grell, G. A., S. Emeis, W. R. Stockwell, T. Schoenemeyer, R. Forkel, J. Michalakes, R. Knoche, W. Seidl, 2000: Application of a multiscale, coupled MM5/chemistry model to the complex terrain of the VOTALP valley campaign. *Atmos. Env.* **34** 1435-1453.

Guenther, A. B., P. R. Zimmerman, P. C. Harley, R. K. Monson, and R. Fall, 1993: Isoprene and monoterpene emission rate variability: Model evaluations and sensitivity analyses. *J. Geophys. Res.*, **98D**, 12609-12617.

Guenther, A., P. Zimmerman, and M. Wildermuth, 1994: Natural volatile organic compound emission rate estimates for U.S. woodland landscapes. *Atmos. Env*., **28**, 1197-1210.

Hahn, J., J. Steinbrecher, and R. Steinbrecher, 1994: Studie F: Emission von Nicht-Methan-Kohlenwasserstoffen aus der Landwirtschaft. In: Enquete-Kommission 'Schutz der Erdatmosphaere' des Deutschen Bundestages (Hrsg.), Studienprogramm Band 1 'Landwirtschaft', Teilband 1 , Economica Verlag, Bonn.

Hirsch, A.I., J.W. Munger, D.J. Jacob, L.W. Horowitz, and A.H. Goldstein, 1996: Seasonal variation of the ozone production efficiency per unit NOx at Harvard Forest, Massachusetts, , *J. Geophys. Res.*, 101, 12,659-12,666.

Jones, A., D. L. Roberts, A. Slingo, 1994: A climate model study of indirect radiative forcing by anthropogenic sulphate aerosols. *Nature,* **370,** 450-453.

Joseph, J. H., W. J. Wiscombe, J. A. Weinmann, 1976: The delta-Eddington approximation for radiative flux transfer. *Journal of Atmospheric Science,* **33,** 2452-2458.

Kulmala, Laaksonen, Pirjola, 1998: Parameterization for sulphuric acid/water nucleation rates, *Journal of Geophysical research*, 103, 8301-8307.

Madronich, S., 1987: Photodissociation in the atmosphere, 1, actinic flux and the effects of ground reflections and clouds. *Journal of Geophysical Research,* **92,** 9740-9752.

McKeen, S.A., B. Eder, G.A. Grell, J. McHenry, A. Stein, and W.M. Angevine, 2003: Evaluation of prototype air quality forecast models – chemistry, NOAA/OAR report.

Middleton, P., W. R. Stockwell, and W. P. L. Carter, 1990: Aggregation and analysis of volatile organic compound emissions for regional modeling. *Atmos. Env.*, **24A**, 1107-1133.

Munger, J.W., S.-M. Fann, P.S. Bakwin, M.L. Goldstein, A.H. Goldstein, A.S. Colman, and S.C. Wofsy, 1998: Regional budgets for nitrogen oxides from continental sources: Variations of rates for oxidation and deposition with season and distance from source regions, *J. Geophys. Res.*, 103, 8355-8368.

Odum, J. R., T. Hoffmann, F. Bowman, D. Collins, R.C. Flagan and J.H. Seinfeld, 1996: Gas/particle partitioning and secondary organic aerosol yields, *Environ. Sci. Technol.*, **30**, 2580– 2585.

Pleim, J. E., A. Venkatram, and R. Yamartino, 1984: *ADOM/TADAP Model Development Program,* Vol. 4. *The Dry Deposition Module*, Ont. Min. of the Environment, Canada.

Ruggaber, A., R. Dlugi, T. Nakajima, 1994: Modeling of radiation quantities and photolysis frequencies in the troposphere. *Journal of Atmospheric Chemistry,* **18,** 171-210.

Satoh, M., 2002: Conservative scheme for the compressible nonhydrostatic models with the horizontally explicit and vertically implicit time integration scheme, *Mon. Wea. Rev.*, **130**, 1227-1245, 2002.

Saxena, P., A.B. Hudischewskyj, C. Seigneur, and J.H. Seinfeld, 1986: A comparative study of equilibrium approaches to the chemical characterization of secondary aerosols, *Atmos. Env*., **20,** 1471-1483.

Schell B., I. J. Ackermann, H. Hass, F. S. Binkowski, and A. Ebel, 2001: Modeling the formation of secondary organic aerosol within a comprehensive air quality model system, *Journal of Geophysical research*, **106**, 28275-28293.

Schoenemeyer, T., K. Richter, and G. Smiatek, 1997: Vorstudie uber ein raumlich und zeitlich aufgelostes Kataster anthropogener und biogener Emissionen fuer Bayern mit Entwicklung eines Prototyps und Anwendung fur Immissionsprognosen. Abschluss bericht an das Bayerische Landesamt fur Umweltschutz. Fraunhofer-Institut fuer Atmosphaerische Umweltforschung, Garmisch-Partenkirchen.

Simpson, D., A. Guenther, C. N. Hewitt, and R. Steinbrecher, 1995: Biogenic emissions in Europe. 1. estimates and uncertainties. *J. Geophys. Res.*, **100D**, 22875-22890.

Slingo, A., 1989: A GCM parameterization for the shortwave radiative properties of water clouds. *Journal of the Atmospheric Sciences,* **46,** 1419-1427.

Slinn, S. A. and W. G. N. Slinn, 1980: Prediction for particle deposition on natural waters, *Atmos. Env.*, **14**, 1013-1016.

Stockwell, W. R., P. Middleton, J. S. Chang, and X. Tang, 1990: The second generation regional acid deposition model chemical mechanism for regional air quality modeling. *J. Geophys. Res.*, **95**, 16343-16367.

Stockwell, W.R., F. Kirchner, M. Kuhn, and S. Seefeld, 1997, A new mechnism for regional atmospheric chemistry modeling, *J.of Geophys .Res.*, 102, 15847-25879.

Weseley, M. L., 1989: Parameterization of surface resistance to gaseous dry deposition in regional numerical models. *Atmos. Env.*, **16**, 1293-1304.

Wicker, L. J., and W. C. Skamarock, 2002: Time splitting methods for elastic models using forward time schemes. *Mon. Wea. Rev.*, **130**, 2088-2097.

Whitby, E.R., P.H. Mcmurry, U. Shankar, and F.S. Binkowski, 1991: Modal Aerosol dynamics modeling, Rep. 600/3-91/020, Atmos. Res. and Exposure Asess. Lab., U.S. Environ. Prot. Agency, Research Triangle Park, N.C., 1991 (Available as NTIS PB91-1617291AS from Natl. Tech. Inf. Serv., Springfield, Va).